



## Effectiveness of cyclic pushover analysis in the prediction of seismic response of steel MRFs

Francesca Barbagallo<sup>1</sup>, Melina Bosco<sup>2</sup>, Aurelio Ghersi<sup>3</sup>, Edoardo M. Marino<sup>4</sup>, Pier Paolo Rossi<sup>4</sup>

<sup>1</sup> Assistant Researcher, Department of Civil Engineering and Architecture, University of Catania - Catania, Italy.

<sup>2</sup> Assistant Professor, Department of Civil Engineering and Architecture, University of Catania - Catania, Italy.

<sup>3</sup> Full Professor, Department of Civil Engineering and Architecture, University of Catania - Catania, Italy.

<sup>4</sup> Associate Professor, Department of Civil Engineering and Architecture, University of Catania - Catania, Italy.

### ABSTRACT

Nonlinear static methods of analysis were developed to provide a level of accuracy of the seismic response of structures comparable with that of nonlinear dynamic analysis, but with a lower computational burden. Scientific literature offers a variety of nonlinear static methods of analysis, and some of them have also been recommended for the seismic assessment of structures by the American and European seismic codes. Although these methods of analysis are generally deemed accurate for the assessment of plane frames where the contribution of a single mode of vibration is significant, they are applied with a monotonically increasing lateral load and thus neglect the cumulative damage that occurs in the structural members due to repeated loading cycles. Because of this, they tend to overestimate the strength and stiffness, and generally underestimate the prediction of the displacement demand. To overcome this drawback, this paper investigates the possibility of conducting a Cyclic Pushover Analysis (CPA) to assess the seismic response of structures. To investigate the effectiveness of the CPA, a steel moment resisting frame has been assumed as case study building. The seismic demand of this frame has been determined by CPA and the cyclic response of the case study has been compared to that obtained by nonlinear dynamic analysis. Two sets of accelerograms are adopted to consider accelerograms that are characterised by similar response spectrum but different significant durations.

Keywords: nonlinear analysis, seismic assessment, degradation, cumulative damage, significant duration.

### INTRODUCTION

Structural members subjected to strong ground motions generally experience inelastic deformations. Because of this, an accurate prediction of the seismic performance of structures requires the explicit determination of the inelastic response of the structure. To this end, the nonlinear dynamic analysis is widely recognised as the best tool to predict the seismic behaviour of structures. Unfortunately, this type of analysis is not suitable for an extensive application for professional purposes, because it involves high computational cost, it is time consuming and its effectiveness is influenced by different aspects, such as the modelling adopted to simulate the cyclic response of structural elements as well as the selection of the ground motions [1,2]. In the last decades, the scientific research has developed an alternative tool, i.e. the nonlinear static method of analysis, which could provide an accurate prediction of the seismic response of structures with a computational burden lower than that required by nonlinear dynamic analysis [3].

Among the approaches available in scientific literature, the Capacity Spectrum Method (CSM) proposed by Freeman [4] and the N2 Method proposed by Fajfar [5] were pioneering methods and were recommended for the seismic assessment of structures by the American and European seismic codes, respectively. Both methods are based on two main assumptions: (1) the contribution of higher modes of vibration to the seismic response is neglected; (2) the load pattern is determined based on the elastic response of the structure. However, these assumptions are not always realistic and they could lead to inaccuracies in the prediction of the structural response. To improve the effectiveness of nonlinear static analysis, advanced nonlinear static methods of analysis have been formulated in the latest decades. Among others, Chopra and Goel [6] developed nonlinear static methods of analysis with multimodal character, while Antoniou and Pinho [7] proposed an adaptive variant. Even more advanced approaches have been proposed recently: e.g. the adaptive capacity spectrum method by Ferraioli et al. [8] and the Advanced N1 method by Lenza et al. [9].

A basic assumption shared by the nonlinear static methods of analysis is that the seismic response of structural elements subjected to earthquake loading can be represented by a curve enveloping the cyclic hysteretic behaviour. In fact, all the previously mentioned nonlinear static methods, even the most advanced, perform the pushover analysis by applying a monotonic lateral load. However, every earthquake input is far from being a monotonic input and is characterized by several

repeated loads with reverse in signs. Further, every structural member has a durable memory of past damages caused by the previous loading cycles, and at any time it will remember all the preceding excursions that contributed to its deterioration. Thus, the strength and deformation capacities of structures are usually related to the cumulative damage. However, this aspect is neglected by the conventional monotonic approaches, which generally overestimate the strength and stiffness of structural members and may lead to an underestimated prediction of the displacement demand.

To overcome this shortcoming, this paper investigates the possibility that the Cyclic Pushover Analysis (CPA) proposed by Panyakapo [10] may be used as a tool for seismic assessment of structures. In the CPA, the structure is subjected to the distribution of horizontal forces that reverses in sign every time a predetermined value of peak displacement is attained. The change of sign of the lateral forces repeats in cycles, which are previously determined according to a loading protocol. Thus, the structural response is represented by a cyclic loop, which is enveloped by a backbone curve. Because of the cyclic approach, the CPA can simulate more realistically the cyclic character of an earthquake loading and it can capture the deterioration of structural members. The benefit that can be provided by the CPA in predicting the seismic response of the structure is also related to the characteristics of the ground motion. In fact, a previous study [11] dealing with structures with degrading characteristics has shown that the ground motion duration, the number of repeated loading cycles, the intensity and frequency content of the ground motion affect the structural collapse. Furthermore, the structural performance depends on the history of previous damaging cycles, which progressively have reduced the stiffness and strength of structural components. Hence, the selected properties of the loading protocol, i.e. number and amplitude of loading cycles, loading steps and control parameter, play a key role to reach a likely and not too conservative estimate of the seismic response.

To investigate the effectiveness of the CPA in predicting the structural response, a steel moment resisting frame is designed and assumed as a case study building. To take into account the cyclic deterioration of structural components, a fibre-based hinge damage accumulation model [12] of this frame is developed using OpenSees software. The seismic demand of this frame is determined by the CPA following the SAC loading protocol [13]. The cyclic response thus obtained is enveloped by the corresponding backbone curve. Furthermore, the seismic demand of the case study frame is determined by Incremental nonlinear Dynamic Analysis (IDA). The results of the CPA are validated by assuming the response obtained by the IDA as target. To this end, the seismic response of the steel frame is determined in terms of global (base shear, top displacement, peak ground acceleration (PGA)), local (storey drift) and cross section (bending moment and curvature, damage index) response parameters.

## CYCLIC PUSHOVER ANALYSIS

The most important feature of the CPA is the cyclic approach of the loading pattern. During the CPA the forces are applied in one direction (e.g. positive) and scaled until a predetermined displacement is attained. Then, the load distribution is reversed and increased again until the second peak displacement is reached. This back-and-forth loading is repeated in cycles, according to the selected loading protocol. The goal is to replicate the load and deformation histories induced in the structure and/or in its components by an earthquake. Unfortunately, no loading protocol can reproduce exactly the deformation histories experienced by the structural members subjected to earthquakes, because the damage cumulated by the structure depends on several aspects, such as the intensity and frequency content of the ground motion, the configuration, strength, stiffness, and modal properties of the structure or the deterioration characteristics of the structural systems and its components. Hence, to come up with a loading history that is conservative but statistically representative of ground motions and structural configurations, scientific literature and codes provisions have proposed a variety loading protocols (e.g. Clark et al. [15], Krawinkler et al. [16]), ATC-24 [14], AISC [13], ASTM [17], FEMA [18]). In this paper, the SAC loading protocol [13] has been adopted to run the CPA. This protocol was developed according to a statistical study [16] conducted on the number and amplitude of storey drift cycles of two steel moment frames. Thus, the amplitude control parameter adopted in this protocol is the storey drift angle. The SAC protocol is composed of three initial groups of cycles (each made of six loading cycles), that push the structure to a storey drift angle equal to 0.0025 rad, 0.0050 rad and 0.0075 rad, respectively. The following four loading cycles lead the structure to a storey drift angle equal to 0.01 rad. The protocol concludes with further loading cycles that increase the storey drift angle attained in the previous loading cycle of 0.005 rad until the failure. Figure 1 (a) shows the SAC loading protocol in terms of top displacement, i.e. storey drift angle times the total height of the frame ( in this case 9.9 m).

Because of the cyclic loading pattern, the seismic response provided by the CPA is cyclic. To determine a single pushover curve, generally in terms of base shear  $V_b$  versus top displacement  $D_t$ , the cyclic response needs to be enveloped by the so called backbone curve, which is characterised by a softening branch caused by the cyclic degradation.

To determine the backbone curve the three following steps are required: (1) evaluation of the top displacement corresponding to the first yielding of the structure; (2) determination of the elastic branch; (3) determination of the plastic branch. The yielding displacement  $D_y$  (step 1) is evaluated from the performance curve ( $V_b - D_t$ ) of the considered structure determined by a conventional monotonic pushover analysis preliminarily run. In this paper, the monotonic pushover analysis was conducted by applying a distribution of forces proportional to the first mode of vibration. Given the performance curve, the yielding

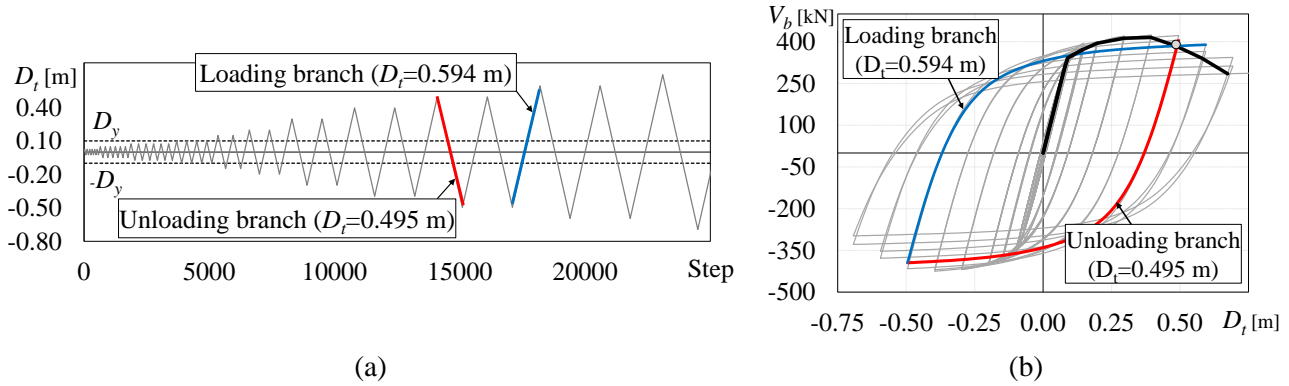


Figure 1. (a) SAC Loading protocol (b) Cyclic response and determination of the generic point of the backbone curve.

displacement  $D_y$  is assumed equal to the top displacement corresponding to a tangent stiffness lower than 80% of the initial elastic stiffness. As long as the structure is pushed towards a top displacement lower than  $D_y$ , the structure remains elastic and the elastic branch of the backbone curve (step 2) retraces the cyclic response. To evaluate the other points of the backbone curve (step 3), it is necessary to identify the first loading branch and the first unloading branch for each considered amplitude of displacement  $D_i$ . The points of the backbone curve following the yielding (step 3) are determined as intersection between the first unloading branch of the cycles at amplitude  $D_{i-1}$  and the first loading branch of the cycles that go to a level of displacement  $D_i$  larger than  $D_{i-1}$ .

Figure 1 (b) shows an example of construction of the backbone curve. The SAC loading protocol is shown in Figure 1(a) and the cyclic response is plotted in Figure 1(b) with the grey line. The first four groups of loading cycles push the structure to top displacements lower than  $D_y$ , which is indicated by the dashed grey line in Figure 1 (a). So far, the backbone curve (black line) follows the cyclic response, as shown in Figure 1(a). The following group of cycles pushes the structure to top displacements larger than  $D_y$ . In this example the top displacement equal to 0.495 m is considered. The red line in Figure 1(a) indicates the first unloading branch of this group of loading cycles. The cyclic response obtained during this unloading branch is plotted in red in Figure 1(b). The blue line in Figure 1 (a) identifies the first loading branch of the group of loading cycle that pushes the structure to a top displacement (0.594 m) larger than that attained by the previous cycle (0.495 m). The corresponding cyclic response is plotted in blue in Figure 1 (b). The intersection between the unloading branch of the previous loading cycle (red line) and the loading branch of the following loading cycle (blue line) is the point of the backbone curve and is indicated by the grey dot. With this procedure, all the points of the backbone curve following the first yielding are obtained Figure 1 (b).

## CASE STUDY BUILDING

The case study building has been designed following the provisions of EC8 [19] for steel moment resisting frames. The building is rectangular in plan ( $19.5 \times 32.5 \text{ m}^2$ ) and the mass at each storey is equal to 193.8 t. The building is three storey high and the interstorey height  $h$  is 3.3 m. The structural scheme is composed of six frames with three spans along the longitudinal directions, and four frames with five spans along the transversal direction. Each span is 6.5 m long, columns are continuous in elevation and oriented as shown in Figure 2 (a). The seismic forces are sustained, both in the  $x$  and  $y$  direction, by the two three-spans external moment resisting (MR) frames (remarked in Figure 2 (a) by a thick line). All the other frames are designed to sustain gravity loads only and beam-to-column connections are pinned. The design internal forces of the MR frames are the sum of those produced by the gravity loads for the seismic design combination (denoted by subscript "G") and those produced by the seismic forces (denoted by subscript "E"). The gravity load for the seismic design combination is equal to  $6.0 \text{ kN/m}^2$  and is determined considering characteristic values of dead and live loads equal to  $g_k = 5.4$  and  $q_k = 2.0 \text{ kN/m}^2$ , respectively, and a combination coefficient  $\Psi_E$  equal to 0.3. In the non-seismic design combination, the sum of the vertical dead and live loads is  $10.56 \text{ kN/m}^2$ , assuming partial safety coefficients  $\gamma_g$  and  $\gamma_q$  equal to 1.4 and 1.5, respectively. The internal forces due to the seismic action are evaluated by the modal response spectrum analysis with the elastic response for soil type A scaled to a peak ground acceleration of 0.15 g. The behaviour factor is assumed equal to 5.

Beams are designed to have plastic moment resistance  $M_{pl,Rd}$  not lower than the design bending moment  $M_{Ed}$ . Furthermore, the cross sections are sized to prevent the decrease of plastic moment resistance and rotation capacity at the plastic hinge because of the design shear and axial forces. To this end, the relevant capacity design criterion is applied according to the following inequalities

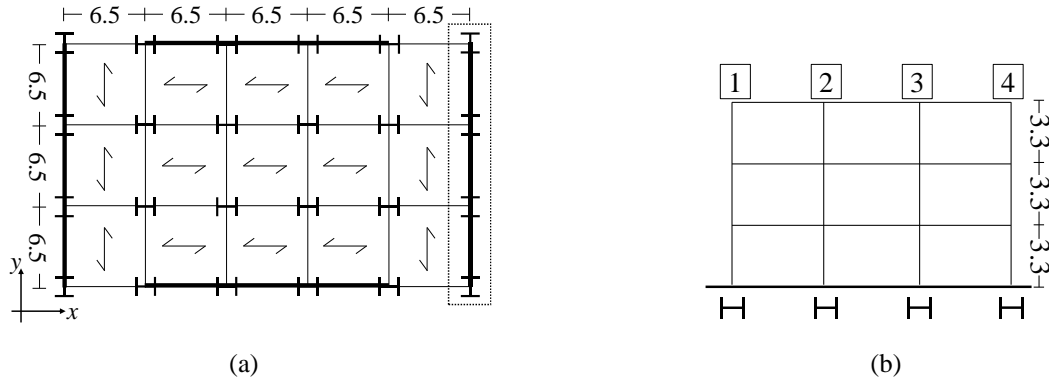


Figure 2. (a) Plan layout of the building; (b) case study frame.

$$V_{Ed} = V_{Ed,G} + V_{Ed,M} \leq 0.5V_{pl,Rd}, \quad N_{Ed} \leq 0.15N_{pl,Rd} \quad (1)$$

$V_{Ed,G}$ ,  $V_{Ed,M}$  and  $V_{pl,Rd}$  being the shear force in the beam due to the gravity loads, the shear force in the beam caused by the application of the moment  $M_{pl,Rd}$  of the beam with opposite sign at the two ending cross sections of the beam, and the shear resistance of the beam, respectively. Further,  $N_{pl,Rd}$  is the plastic axial resistance and  $N_{Ed}$  is the design axial force. The overstrength factor of the beams is evaluated [20] as the minimum of the following ratio in all the beams of the frame

$$\Omega_{min} = \frac{M_{pl,Rd} - M_{Ed,G,i}}{M_{Ed,E,i}} \quad (2)$$

To fulfil the resistance and stability verifications of columns, the design values of bending moment, shear force and axial force are determined by the following relations, which put into effect the capacity design for columns

$$N_{Ed} = N_{Ed,G} + 1.1\gamma_{ov}\Omega_{min} N_{Ed,E} \quad (3)$$

$$M_{Ed} = M_{Ed,G} + 1.1\gamma_{ov}^2\Omega_{min} M_{Ed,E} \quad (4)$$

$$V_{Ed} = V_{Ed,G} + 1.1\gamma_{ov}\Omega_{min} V_{Ed,E} \quad (5)$$

The previous equations are not applied in the case of the bottom and top cross section of the columns of the first and top storey, respectively. Indeed, the design bending moment of those columns are obtained from the structural analysis. To ensure the ductility of columns of the first storey, their size is selected so that the axial force and the shear force be lower than 30% of the plastic axial resistance and 50% of the plastic shear resistance, respectively.

For the MR frame, the cross sections of columns are HEB 220, with the exception of the two interior columns (column 2 and 3 in Figure 2 (b)) at the first and second storey, whose cross section is HEB 260. At all storeys of the MR frame, the cross section of beams is IPE 300. For the interior frames with pinned connections, columns and beams are designed to sustain gravity loads only and the adopted cross sections are HEB 200 and IPE 400, respectively.

### SEISMIC ASSESSMENT OF THE CASE STUDY FRAME AND VALIDATION OF THE CPA

The effectiveness of the CPA in predicting the seismic response of the designed steel frame has been evaluated. To this end, a numerical model of the case study building was built in OpenSees [22] and the structural response was determined by CPA, following the SAC loading protocol. The cyclic response thus obtained has been enveloped by the backbone curve according to the procedure shown before. Further, each value of the displacement demand is associated with the corresponding Peak Ground Acceleration (PGA) according to the Capacity Spectrum Method [4] using the elastic spectrum proposed by EC8 for soil type C. The seismic response determined by CPA is compared with the response evaluated by IDA, assumed as the target response. To this end, two sets of ten artificial accelerograms, generated by the SIMQKE computer program [21] and compatible with the assumed elastic response spectrum, are used. To cover a wide range of effective durations, the accelerograms belonging to the two sets are characterized by different effective durations. The values of PGA are increased from 0.05 g to 1.20 g in steps of 0.05 g. A Rayleigh viscous damping is used and set at 5% for the first two modes of vibration.

The stiffness coefficient of the Rayleigh formulation is applied to the tangent stiffness matrix of the elements.  $P-\Delta$  effects are not included in the numerical analyses to avoid extra sources of degradation.

### Numerical model

The considered frame is three storey high and three span wide and it is the external frame in the  $y$  direction (Figure 2). Columns and beams of the case study frames are modelled by means of *beam with hinges* elements, where the central part is elastic and the inelasticity is concentrated in the plastic hinge segments at the two ends. Within the plastic hinge length, the cross section is subdivided into fibres.

Since capacity design principles were applied, a significant inelastic behaviour is expected in beams, while a moderate inelastic behaviour is expected in columns. For this reason, the degradation of stiffness and strength due to nonlinear cyclic behaviour is considered only for beams, and not for columns. The cross sections of columns are modelled by means of five fibres for each flange, five fibres for the web and four additional fibres for the root fillets. Instead, to simulate the degradation of stiffness and strength in beams due to local buckling of I-shape flanges, the numerical model proposed by Bosco and Tirca [12] is assigned to the flange fibres of beam. According to this model, each flange of the I-shape cross section is divided into 30 segments and 4 layers (30 x 4), while the web is discretized into 30 layers. To simulate the response of steel, the uniaxial model by Menegotto and Pinto (Steel02) [23] is assigned to fibres. With regards to the parameters that control this model [26], the strain hardening ratio is assumed equal to 0.0030 and the coefficient  $R_0$  is set equal to 20. Coefficients  $c_{R1}$  and  $c_{R2}$  are assumed equal to 0.925 and 0.15, respectively, as proposed in OpenSEES manual [22]. No isotropic hardening is considered. The yield strength  $F_y$  and the Young modulus  $E$  are equal to 235 MPa and 210000 MPa, respectively. This material model is able to take into account the accumulated plastic deformation at each point of load reversal. Accordingly, each hysteretic loop follows the previous loading path for a new reloading curve, while deformations accumulate. The low-cycle fatigue material is combined with Steel02 material assigned to fibres of the plastic hinge zones. The fatigue material (uniaxialMaterial Fatigue) already implemented in OpenSees uses an accumulative strain model to predict damage in accordance with the Miner's rule. The relationship between the plastic strain amplitude experienced at each cycle and the number of cycles to failure is that proposed by Coffin and Manson. The fatigue ductility exponent  $m$  is equal to -0.5. To simulate the gradual stiffness and strength degradation caused by local buckling, the fatigue coefficient  $\epsilon_0$  is assigned to flange fibres according to a linear distribution [12]. In particular, a minimum value  $\epsilon_{0,min}$  is assigned to fibres located at the edges of both flanges and a maximum value ( $\epsilon_{0,min} + \Delta\epsilon_0$ ) is assigned to flanges fibres located at the intersection with the web. The term  $\epsilon_{0,min}$  is related to the initiation of local buckling, and it is here assumed equal to 0.029, according to the value suggested in [12]. The term  $\Delta\epsilon_0$  controls the rate of degradation and it is here assumed equal to 0.0835. Further details about the numerical model can be found in reference [12]. The length of the plastic hinge is set equal to  $0.22 L_V$ , where  $L_V$  is the shear length evaluated as the ratio of the bending moment to the shear force

### Seismic input

Two sets of ten artificial accelerograms generated by the computer program SIMQKE [21] were adopted as seismic inputs. Each accelerogram is defined by stationary random process modulated by a compound intensity function [24]. The earthquake rise time is 5.0 s, the parameter IPOW of the first branch and the parameter ALFA0 of the third one are assumed equal to 2.0 and 0.25, respectively. The stationary phase is followed by a latter 15 s phase with decreasing values of accelerations. Details regarding the envelope intensity function and the procedure for the determination of the length of the parts of the compound function may be found in [24]. The two sets are hereinafter named Long Set (LS) and Short Set (SS). Each accelerogram of LS and SS is characterized by a total duration  $T_t$  equal to 90 s and 27 s, and a duration of the stationary part  $T_s$  equal to 70 s and 7 s, respectively. For each accelerogram, the value of the Arias Intensity AI has been calculated. The significant duration of each ground motion, denoted as 5-95%  $D_s$ , has been determined as the interval between the times at which 5% and 95% of the Arias Intensity of the ground motion have been recorded, i.e. the duration of time over which the 90% of the energy is accumulated [11]. Given the values for the total duration and the stationary part duration, the mean value of 5-95%  $D_s$  over the

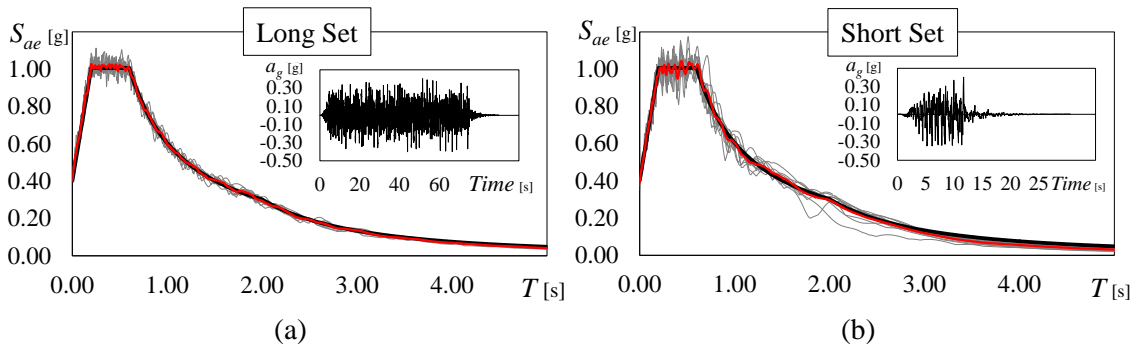


Figure 3. Elastic spectra of the selected accelerograms: (a) Long Set (LS), (b) Short Set (SS).

ten accelerograms resulted to be equal to 63.5 s and 7.5 s for LS and SS, respectively. These values are selected so as to cover the range of effective durations reported in [11].

The accelerograms of each set are compatible with the elastic response spectra reported in EC8 for an equivalent viscous damping ratio equal to 5%, PGA equal to 0.35 g and soil type C. The elastic spectra of the selected accelerograms (grey thin lines), the corresponding average response spectra (red line) and the elastic spectrum of EC8 (black thick line) are shown in Figure 3.

### Response parameters

In this section the effectiveness of the CPA is evaluated by comparing the seismic response of the case study frame determined by the CPA with that obtained by the IDA. To this end, the seismic response of the case study frame has been determined in terms of both global and local response parameters. The response parameters considered at global level are the top displacement  $D_t$  and the PGA. In the case of IDA, given the value of PGA, the corresponding value of  $D_t$  has been determined by averaging the maximum top displacement recorded for each of the 10 ground motions. In the case of CPA, each point of the pushover curve (i.e. each couple of top displacement demand and base shear of the backbone curve) is associated to the corresponding PGA according to the Capacity Spectrum Method [4], whereby the equivalent damping ratio is evaluated by the equation proposed for steel members in [25].

The seismic response at local level was evaluated based on the distribution of storey drift along the height of the frame. Two limit states were considered in the IDA, i.e. the attainment of a maximum storey drift equal to 2% and 6%. Each limit state corresponds to a value of PGA (PGA2% and PGA6%) and top displacement ( $D_{t,2\%}^{IDA}$  and  $D_{t,6\%}^{IDA}$ ). Fixing the top displacement at the value corresponding to the attainment of the considered limit state in the IDA, the corresponding distribution of storey drift obtained by the IDA has been compared with that evaluated by the CPA when (in the cyclic analysis, not the backbone curve)  $D_t^{CPA} = D_t^{IDA}$ .

The seismic response has also been investigated at cross section level. The damage of the beams is measured by a damage index DI computed for each cross section as the ratio of the number of flanges fibres in which the Miner's damage index is equal to one (i.e. the number of fibres reaching fatigue) to the entire number of flange fibres within a given cross section [12]. When  $DI = 1.0$ , flanges of I-shape beam's cross section are not able to contribute to the plastic resistance of the cross section in the plastic hinge zone. A value of  $DI = 0.375$ , approximately corresponding to the 80% of remaining bending moment capacity of the beam, was assumed to indicate the beam's failure due to low-cycle fatigue [12]. In the case of the CPA, the DI is evaluated at the end of each loading cycle corresponding to the attainment of the top displacement imposed by the adopted loading protocol. Instead, in the IDA the DI is evaluated at the end of each time-history (i.e. of each accelerograms scaled at a given PGA). The obtained values of the DI of each cross section are averaged over the number of accelerograms and are related to the maximum top displacement for the selected PGA. For a comprehensive view of the damage in the frame, the following parameters were evaluated: (1) the  $DI_{av}$ , evaluated as the average of the mean DI of the  $n$  storeys; (2) the  $DI_{max}$  evaluated as the maximum DI over the entire frame. The response parameters were evaluated by the IDA and compared to those obtained by the CPA.

### Validation of the CPA

The seismic response of the designed frame is plotted in terms of PGA and top displacement  $D_t$  in Figure 4 (a). The red continuous line plots the results provided by the CPA. The black and white dots show the results obtained by the Long Set (LS) and Short Set (SS), respectively. Particularly, for each of the three input sets, given the PGA, the corresponding top

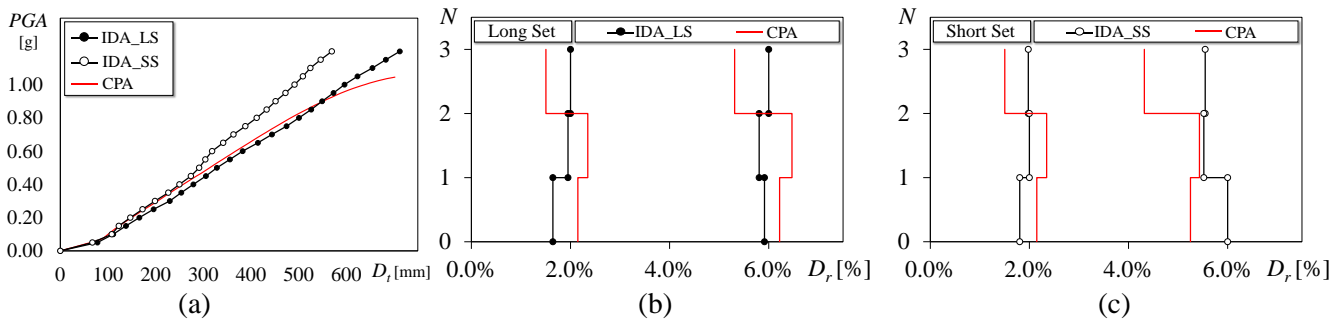


Figure 4: (a) Peak Ground Acceleration Vs Top displacement obtained by CPA and IDA with Long and Short sets; Storey drift distribution obtained by CPA corresponding to the top displacement leading to a maximum drift in the IDA equal to 2% and 6%: (b) LS and (c) SS.

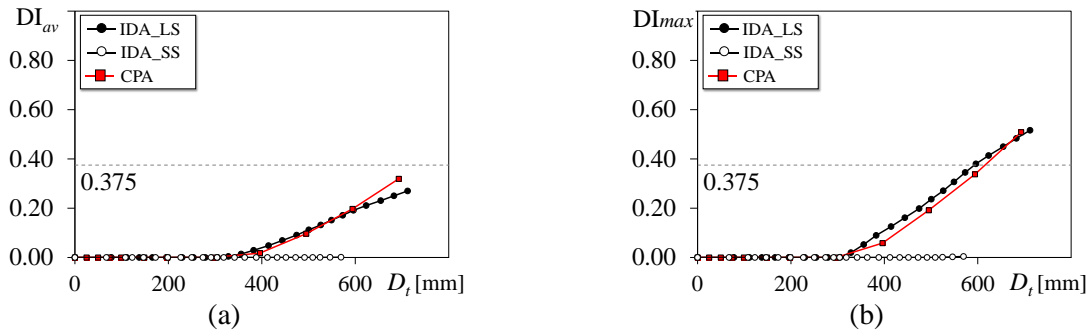


Figure 5. Damage index evaluated by CPA and IDA with Long and Short sets. (a) average  $DI_{av}$ , (b) maximum  $DI_{max}$ .

displacement is the average of the 10 maximum top displacements of the 10 accelerograms. The comparison of these two plots shows that the duration of the input accelerograms affects the seismic response. In fact, given a value of PGA, the SS leads to top displacements significantly lower than those attained under the LS. Thus, if the effective duration of the input accelerogram is short (7.5 s), the stiffness and strength degradation due to the cumulated damage is not significant. On the contrary, when the effective duration of the seismic input becomes significant (63.5 s), the degradation of the cross sections turns into a critical issue. Based on these results, the CPA becomes extremely effective when accelerograms of long duration are considered. In fact, at a PGA equal to 1 g, the CPA estimated the top displacement demand with an error lower than 10%.

Figure 4 (b) and (c) compares the heightwise distributions of storey drifts  $D_r$  evaluated by CPA and IDAs with the long and short input sets, respectively. Two limit states are considered in every IDA: the attainment of a maximum storey drift angle equal to 2% or 6%. The corresponding distributions of storey drifts of the CPA are those corresponding to a top displacement equal to that leading the IDA to the considered limit state. At 2% limit state, regardless of the input set, the CPA overestimates the drifts of the first two storeys and underestimates that of the third storey. However, the CPA identifies correctly the storey where the drift concentration is larger (second storey). When 6% limit state is achieved and the input set has long duration, the CPA still provides a conservative estimate of the drifts.

To validate the CPA at a local level, Figure 5 (a) and (b) compares the average  $DI_{av}$  and the maximum  $DI_{max}$ , respectively, of the entire frame evaluated by CPA and IDAs with LS and SS. In both cases, the SS (white dots) led to almost no damage in the cross sections and the average and the maximum DI were null. The largest damage is attained when the duration of the input is 90 s (black dots). In this case, the damage index keeps a value on average lower than 0.375, owing to the beams of the third floor that basically remain elastic and decrease the average damage index. Instead, the maximum value of the damage index overcomes the limit value, due to the concentration of damage that causes the failure of the beams of the first and second floors. The average and the maximum damage indexes estimated by the CPA (red line) are plotted along with those of the IDAs. This evidences that the enhancement provided by the CPA is fundamental to estimate accurately both the average and the maximum damage index when long duration accelerograms are applied.

## CONCLUSIONS

This paper investigates the use of the Cyclic Pushover Analysis to take into account the degradation of stiffness and strength typically caused by the damage cumulated in cross sections in occurrence of earthquake loading. To this end, a steel moment resisting frame was designed and modelled in OpenSees adopting a fibre-damage accumulation model. The seismic response of this frame was determined by CPA following the loading protocol proposed by SAC. The effectiveness of the CPA was examined through comparison with the incremental nonlinear dynamic analysis. The IDA was conducted considering two sets of input accelerograms with short and long duration, respectively. From the numerical analysis conducted on this model, the CPA showed the capability of catching the stiffness and strength degradation, in particular in the case of long duration earthquakes, when the cross sections of structural components undergo several loading cycles. Indeed, the IDA show that, given a peak ground acceleration, the displacement demand provided by long duration set is significantly larger than that caused by short duration earthquakes. Thus, the CPA was necessary to estimate accurately the response of the structure, particularly in the case of long duration earthquakes. Further, the importance of considering the cyclic deterioration is shown at a local level, by means of the average and the maximum damage index of the frame. In the case of long earthquakes, given a top displacement of 600 mm (corresponding to a PGA equal to 1 g), the CPA estimated the damage indexes with an error equal to 12%.

## REFERENCES

- [1] Christovasilis, P., Cimellaro G.P., Barani, S., Foti, S., (2014). “On the selection and scaling of ground motions for fragility analysis of structures”, In: *Proceedings of 2<sup>nd</sup> European Conference of Earthquake Engineering and Seismology*.
- [2] Gehl, P., Douglas, J., Seyedi, D. M., (2015). “Influence of the Number of Dynamic Analyses on the Accuracy of Structural Response Estimates”, *Earthquake Spectra*, 31, 97-113,.
- [3] Repapis, C.C., (2016). “Seismic performance evaluation of existing RC buildings without seismic details. Comparison of nonlinear static methods and IDA”, *The Open Construction and Building Technology Journal*, 10, 158-179.
- [4] Freeman, S.A., (1998). “The capacity spectrum method as a tool for seismic design”, In: *Proceedings of 11th European Conference on Earthquake Engineering*, Paris, France.
- [5] Fajfar, P., Gaspersic, P., (1996). “The N2 method for the seismic damage analysis of RC buildings”, *Earthquake Engineering and Structural Dynamics*, 25, 31-46.
- [6] Chopra, A.K., Goel, R.K., (2002). “A Modal Pushover Analysis Procedure for Estimating Seismic Demands of Buildings”, *Earthquake Engineering and Structural Dynamics*, 31, 561-582.
- [7] Antoniou, S., Pinho, R., (2004). “Development and verification of a displacement – based adaptive pushover procedures”, *Journal of Earthquake Engineering*, 8, 643- 661.
- [8] Ferraioli, M., Lavino, A., Mandara, A., (2016). “An adaptive capacity spectrum method for estimation seismic response of steel moment resisting frames”, *Ingegneria Sismica*, 33, 47-60.
- [9] Lenza, P., Ghersi, A., Marino, E.M., Pellicchia, M., (2017). “A multimodal adaptive evolution of the N1 method for assessment and design of RC framed structures”, *Earthquake and Structures*, 12, 271-284.
- [10] Panyakapo, P., (2014). “Cyclic pushover analysis procedure to estimate seismic demands for buildings”, *Engineering Structures*, 66, 10-23.
- [11] Raghunandan, M., Liel, A.B., (2013). “Effect of strong motion duration on earthquake-induced structural collapse”, *Structural safety*, 41, 119-133.
- [12] Bosco, M., Tirca, L., (2017). “Numerical simulation of steel I-shaped beams using a fiber-based damage accumulation model”, *Journal of Constructional Steel Research*, 133, 241-255.
- [13] ANSI/AISC 341-05. (2005). Seismic Provisions for Structural Steel Buildings.
- [14] ATC-24, (1992). “Guidelines for Cyclic Seismic Testing of Components of Steel Structures for Buildings”, Report No. ATC-24, Applied Technology Council, Redwood City, CA.
- [15] Clark, P., Frank, K., Krawinkler, H., Shaw, R., (1997). *Protocol for Fabrication, Inspection, Testing, and Documentation of Beam-Column Connection Tests and Other Experimental Specimens*, SAC Steel Project Background Document. Report No. SAC/BD-97/02.
- [16] H. Krawinkler, A. Gupta, R. Medina, N. Luco, (2000). *Development of Loading Histories for Testing of Steel Beam-to-Column Assemblies*, SAC Background Report SAC/BD-00/10, 2000-a.
- [17] ASTM, (2003). “Standard Test Method for Cyclic (Reversed) Load Test for Shear Resistance of Walls for Buildings”, ES 2126-02a.
- [18] FEMA, (2007). “Interim Protocols for Determining Seismic Performance Characteristics of Structural and Nonstructural Components Through Laboratory Testing”, FEMA 461 Draft document, Federal Emergency Management Agency.
- [19] CEN. EN 1998-1, (2004). EuroCode 8: Design of structures for earthquake resistance – Part 1: General rules, seismic actions and rules for buildings. Bruxelles: European Committee for Standardization.
- [20] Elghazouli, A.Y., (2010). “Assessment of European seismic design procedures”, *Bulletin of Earthquake Engineering*, 8, 65-89.
- [21] SIMQKE, (1976). A program for artificial motion generation, User’s manual and documentation, Department of Civil Engineering MIT.
- [22] Mazzoni, S., McKenna, F., Scott, M. H., Fenves, G.L., Jeremic, B., (2003). “OpenSees Command Language Manual”, Pacific Earth. Eng. Research Center, University of California at Berkeley.
- [23] Menegotto, M., Pinto, P.E., (1973). “Method of analysis for cyclically loaded reinforced concrete plane frames including changes in geometry and non-elastic behavior of elements under combined normal force and bending”, In: *Proceedings of IABSE symposium of resistance and ultimate deformability of structures acted on by well-defined repeated loads*, Lisbon, Portugal.
- [24] Amara, F., Bosco, M., Marino, E.M., Rossi, P.P., (2014). “An accurate strength amplification factor for the design of SDOF systems with P-D effects”, *Earthquake Engineering and Structural Dynamics*, 43, 589–611.
- [25] Priestley, M.J.N., (2003). “Myths and fallacies in earthquake engineering”, Revisited, The Mallet Milne Lecture, IUSS Press, Pavia, Italy.